

Fast Thermalization and Helmholtz Oscillations of an Ultracold Bose Gas

D. J. Papoular,^{1,*} L. P. Pitaevskii,^{1,2} and S. Stringari¹

¹*INO-CNR BEC Center and Dipartimento di Fisica, Università di Trento, 38123 Povo, Italy*

²*Kapitza Institute for Physical Problems, Kosygina 2, 119334 Moscow, Russia*

(Received 23 May 2014; published 20 October 2014)

We analyze theoretically the transport properties of a weakly interacting ultracold Bose gas enclosed in two reservoirs connected by a constriction. We assume that the transport of the superfluid part is hydrodynamic, and we describe the ballistic transport of the normal part using the Landauer-Büttiker formalism. Modeling the coupled evolution of the phase, atom number, and temperature mismatches between the reservoirs, we predict that Helmholtz (plasma) oscillations can be observed at nonzero temperatures below T_c . We show that, because of its strong compressibility, the Bose gas is characterized by a fast thermalization compared to the damping time for plasma oscillations, accompanied by a fast transfer of the normal component. This fast thermalization also affects the gas above T_c , where we present a comparison to the ideal fermionic case. Moreover, we outline the possible realization of a superleak through the inclusion of a disordered potential.

DOI: 10.1103/PhysRevLett.113.170601

PACS numbers: 05.60.-k, 03.75.Kk, 67.10.Jn, 67.85.-d

Recent experiments have initiated the exploration of the transport properties of ultracold atomic gases [1–9] in geometries comprising two reservoirs separated by a potential barrier or a constriction (see Fig. 1). The constriction-based geometry presents pluridisciplinary issues related to mesoscopic physics, disorder, and superfluidity. In the context of mesoscopic physics [10], it has been used to observe contact resistance [4], quantized conductance [8], and thermoelectric effects [6,11] in ultracold Fermi gases. The creation of directed atomic currents in between two connected reservoirs makes this geometry relevant for atomtronics [12]. Constriction-based setups have also allowed for the investigation of superflow [5], as well as the exploration of the competition of disorder with superfluidity [9] and with conductance [6].

Constricted geometries hold further promises for atomic superfluids. First, the observation of the fountain effect of superfluid helium [13] relies on the use of a superleak, which lets the superfluid through while blocking the normal part. Superleaks are familiar elements in the context of experiments on helium [14], but their design in the context of ultracold gases remains an open question. Their implementation would allow, for instance, the implementation of new adiabatic cooling schemes [15], the efficient excitation of second sound [14], and, more generally, an advanced control over transport phenomena. Second, superfluids trapped in two connected reservoirs are expected to undergo plasma oscillations, which are analogous to the oscillations of a gas in between two connected Helmholtz resonators (see Ref. [16], Sec. 69). These oscillations have been extensively studied in the context of liquid helium [17]. Similar oscillations have also been observed with ultracold Bose gases in double-well potentials [18,19].

In ultracold Fermi gases, the occurrence of BCS-type superfluidity occurs at reasonably high temperatures only in the presence of strong interactions [20]. In this case, both the superfluid and normal parts of the quantum fluid are deep in the hydrodynamic regime, which affords a strong analogy with superfluid helium [21]. However, it also makes it more difficult to tell the behavior of the superfluid fraction apart from that of the normal fraction. Hence, in the present Letter, we focus on weakly interacting bosonic gases, where the parameters can be chosen such that superfluid transport is hydrodynamic whereas normal transport is ballistic.

Motivated by the possible realization of a superleak, we develop a theory describing the transport properties of weakly interacting uniform Bose gases under these conditions, reflecting the different transport regimes for the superfluid and normal parts. We use it to show that plasma oscillations are observable even at nonzero temperatures below T_c , and we describe the damping mechanism due to the coupling between the superfluid and normal parts. We also show that the large compressibility of the Bose gas leads to surprisingly fast thermalization compared to the damping time of the transport phenomena. This new effect is related to the thermoelectric properties of the gas. Below T_c , it causes an efficient transport of the normal part at short

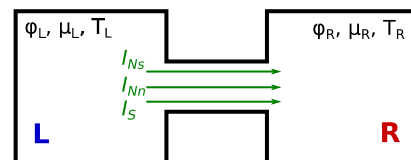


FIG. 1 (color online). Two reservoirs can exchange particles and heat through a constriction.

times; above T_c , it yields a key difference compared to ideal fermionic gases. It hinders the realization of a superleak, which will require an additional ingredient, such as a disordered potential.

We describe the ballistic transport of the normal part using the Landauer-Büttiker formalism for quantum transport [22]. To our knowledge, the present work is the first application of this formalism to massive bosons. It had been applied to (massless) phonons to analyze heat conductance at the quantum level [23].

We assume that the two compartments of Fig. 1 are box traps with the same volume $V^L = V^R$, each enclosing a uniform superfluid. We model the constriction by an isotropic radial harmonic trap of frequency $\omega_\perp/2\pi$. The hydrodynamic assumption for superfluid transport through the constriction (see Ref. [24], Chap. 5) is valid if $\hbar\omega_\perp \ll gn$, where n is the mean gas density inside the constriction, $g = 4\pi\hbar^2 a/m$ is the interaction constant, a is the scattering length, and m is the atomic mass.

We call $\delta N_s = N_s^R - N_s^L$ and $\delta N_n = N_n^R - N_n^L$ the difference in superfluid and normal atom numbers between the right and left compartments of Fig. 1, and $\delta S = S^R - S^L$ the analogous entropy difference. We focus on small deviations from the homogeneous situation. In this linear-response regime, the superfluid current I_{N_s} , the normal current I_{N_n} , and the entropy current I_S , are linear functions of the small differences in phase $\delta\phi$, chemical potential $\delta\mu$, and temperature δT between the two reservoirs, which we write in matrix form as

$$\begin{pmatrix} I_{N_s} \\ I_{N_n} \\ I_S/k_B \end{pmatrix} = \begin{pmatrix} I_J/\omega_\perp & 0 & 0 \\ 0 & L_{11} & L_{12} \\ 0 & L_{12} & L_{22} \end{pmatrix} \begin{pmatrix} \hbar\omega_\perp \delta\phi \\ \delta\mu \\ k_B \delta T \end{pmatrix}. \quad (1)$$

Equation (1) generalizes the 2×2 matrix introduced in Ref. [6] in the absence of superfluid. The first line of Eq. (1) reflects the definition of the superfluid current, $\mathbf{j}_s = n_s \mathbf{v}_s$, where n_s is the mean superfluid density in the reservoirs, and $\mathbf{v}_s = \hbar \nabla \phi / m$ is the superfluid velocity. For the geometry of Fig. 1, $I_J = 2n_s A / ml$, where l is the constriction length and $A = \pi g n_s / m \omega_\perp^2$ is its effective Thomas-Fermi section. The two zeros in the first column reflect the fact that the normal-part quantities δN_n and δS do not explicitly depend on $\delta\phi$. The coefficients (L_{ij}) describe the ballistic transport of the normal part and the entropy. The normal part consists of the thermal excitations present in the gas. Assuming that $k_B T \gg gn$, these are particles, and an analysis of the role of interactions using Hartree-Fock theory reveals that the ideal-gas expressions for the L_{ij} 's are applicable. This assumption on T rules out low-temperature collective phenomena, such as anomalous phonon transmission [25] or Andreev reflection [26]. For uniform Bose gases, it is easy to satisfy while maintaining the presence of superfluid ($T < T_c$), because the ratio $gn/k_B T_c$ is of the order of 0.04.

We calculate the L_{ij} 's using the Landauer-Büttiker formalism (see Ref. [22], Chap. 2). We describe the excitations in each reservoir using Bose distributions η^B , whose difference $\delta\eta^B = \eta_R^B - \eta_L^B = \partial\eta^B/\partial\mu|_T \delta\mu + \partial\eta^B/\partial T|_\mu \delta T$. For $T < T_c$, the L_{ij} 's are given by [27]

$$hL_{11} = -\frac{\pi^2}{6} \left(\frac{k_B T}{\hbar\omega_\perp} \right)^2, \\ L_{12} = L_{21} = \frac{18}{\pi^2} \zeta(3) L_{11}, \quad L_{22} = \frac{4\pi^2}{5} L_{11}, \quad (2)$$

where h is Planck's constant. The L_{ij} 's do not depend on l ($\sim 5 \mu\text{m}$), because it is much shorter than the thermal mean free path inside the reservoirs ($\sim 100 \mu\text{m}$). Furthermore, the L_{ij} 's all share the same dependence on T and ω_\perp . This second property is an important difference with respect to the fermionic case [6], where the chemical potential is of the order of the Fermi energy and, hence, enters in the expression for the transport coefficients.

The coupling between the superfluid and normal parts arises from the equation of state, which involves the total gas density in each reservoir, e.g., $n^R = (N_s^R + N_n^R)/V^R$, and from the equation for the superfluid velocity, $\hbar\partial_t \delta\phi = -\delta\mu$ [24]. Combining these equations with Eq. (1), we obtain a differential system describing the evolution of $\delta\phi$, δN , and δT [28],

$$\tau_1 \frac{d}{dt} \begin{pmatrix} \frac{\hbar\delta\phi}{\tau_1} \\ \frac{\delta N}{\kappa_T} \\ k_B \delta T \end{pmatrix} = \begin{pmatrix} 0 & -1 & 0 \\ (\omega_{\text{pl}}\tau_1)^2 & -1 & +\mathcal{S} \\ 0 & \mathcal{S}/\ell & -\tau_1/\tau_T \end{pmatrix} \begin{pmatrix} \frac{\hbar\delta\phi}{\tau_1} \\ \frac{\delta N}{\kappa_T} \\ k_B \delta T \end{pmatrix}. \quad (3)$$

In Eq. (3), $\kappa_T = \partial N/\partial\mu|_T$ is the isothermal compressibility, $C_N = T\partial S/\partial T|_N$ is the heat capacity, $\ell = C_N/\kappa_T T$ is their ratio, and the Seebeck coefficient $\mathcal{S} = -\partial\mu/\partial T|_N - L_{12}/L_{11}$ encodes the thermoelectric properties of the gas. Equation (3) introduces three time scales,

$$\tau_1 = \frac{\kappa_T}{-L_{11}}, \quad \tau_{\text{pl}} = 2\pi\sqrt{\frac{\kappa_T}{I_J}}, \quad \tau_T = \frac{C_N/T}{-L_{22}}, \quad (4)$$

where τ_1 is related to normal transport and determines the damping of plasma (pl) oscillations and thermoelectric effects, the bare plasma period $\tau_{\text{pl}} = 2\pi/\omega_{\text{pl}}$ is related to superfluid transport, and τ_T is the thermalization time (see Fig. 2).

Weakly interacting Bose gases are characterized by a very large compressibility ($\kappa_T = N/gn$ for $T < T_c$), whereas C_N/Nk_B is finite (see Fig. 3, left). Hence, the ratio ℓ is very small, of the order of a few 10^{-2} , which is a key difference with respect to ideal Fermi gases ($\ell \sim 1$, Fig. 3, center) and liquid helium 4 ($\ell \sim 10$ near the superfluid transition, Fig. 3, right). This specific property of Bose gases leads to $\tau_T \ll \tau_1$; i.e., thermalization is much faster than the damping due to normal transport.

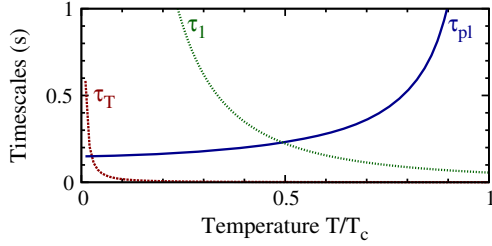


FIG. 2 (color online). The time scales τ_T (dashed red line), τ_{pl} (solid blue line), τ_1 (dotted green line), for a ^{87}Rb gas with $n = 10^{19}$ atoms/m 3 , $N = 10^5$ atoms in each reservoir, $\omega_{\perp}/2\pi = 15$ Hz and $l = 5$ μm .

Furthermore, if T is high enough for the Hartree-Fock theory to hold ($k_B T \gtrsim$ a few gn), but low enough for the superfluid fraction $N_s/N = 1 - (T/T_c)^{3/2}$ to be substantial ($T/T_c \lesssim 0.5$), the time scales satisfy $\tau_T \ll \tau_{pl} < \tau_1$. On the other hand, if $T \gtrsim T_c$, the superfluid is absent and our description reduces to the coupled system on δN and δT introduced in Ref. [6], corresponding to the lower right 2×2 block of the matrix in Eq. (3).

Plasma oscillations.—We now turn to the analysis of plasma oscillations in the geometry of Fig. 1. These oscillations can be excited by introducing an initial atom number mismatch δN between the two reservoirs. We have predicted their occurrence at $T = 0$ by numerically solving the Gross-Pitaevskii equation, using a Crank-Nicolson scheme [30,31]. We have investigated the 2D geometry represented in Fig. 1, as well as the corresponding cylindrically symmetric three-dimensional geometry, choosing the linear size of the reservoirs and the atomic density in each reservoir to be of the same order of magnitude as in Ref. [32]. Our results show that the quantum pressure term in the Gross-Pitaevskii equation (see Ref. [24], Sec. 5.2) is negligible for typical values of the density, reservoir volumes, and constriction radius, which validates the hydrodynamic approach for superfluid transport. They confirm that zero-temperature oscillations occur at the Helmholtz frequency $\omega_{pl}^{(0)}$ (see Ref. [16], Sec. 69), which is of the order of a few Hz and, hence, amenable to observation.

Our model allows us to investigate plasma oscillations at nonzero temperatures. First, our Hartree-Fock description shows that the bare plasma frequency ω_{pl} scales with $a/l^{1/2}$, whereas the damping factor $\omega_{pl}\tau_1$ is proportional to $(T_c/T)^2/\sqrt{l}$ and does not depend on a . Therefore, the observation of oscillations will be favored by using smaller constriction lengths, lower temperatures T/T_c , and larger scattering lengths a . Plasma oscillations occur if the matrix entering Eq. (3) has two complex-conjugate eigenvalues with negative real parts, $(-1/\tau_{\text{damp}} \pm i\omega_{\text{osc}})$. Then, the plasma frequency is $\omega_{\text{osc}}/2\pi$ and the damping time is τ_{damp} . Figure 4, left, shows the dependence of ω_{osc} and τ_{damp} on T/T_c for a typical ^{87}Rb gas below T_c . Oscillations occur for $T \lesssim 0.95T_c$. For higher temperatures, the superfluid fraction is negligible, and the damping time coincides with that predicted by the normal-part model of Ref. [6].

Thermalization being a fast process compared to the time scales τ_{pl} and τ_1 causes the evolution of δT to approximately decouple from that of $\delta\phi$ and δN . Hence, the dynamics of these latter two quantities is almost isothermal and is piloted by the upper left 2×2 block of the matrix entering Eq. (3). The maximum amplitude of the temperature oscillations can be determined by assuming that the dynamics of δT is driven by that of δN and $\delta\phi$:

$$\frac{\delta T_{\text{max}}}{T} = \frac{gn}{k_B T} \frac{S}{S^2 + L} \frac{\delta N_0}{N}, \quad (5)$$

where $L = L_{22}/L_{11} - (L_{12}/L_{11})^2$. The presence of the factor $gn/k_B T$ in Eq. (5) keeps $\delta T_{\text{max}}/T$ small and confirms the near-isothermal nature of these oscillations. Figure 4, left, shows that the frequency and damping time predicted by the isothermal model (green) agree with the full calculation (red). Hence, the main decay mechanism is due to the presence of the normal part. Thermoelectric effects, neglected in the isothermal model, mostly affect the damping time, causing it to lengthen.

The plasma oscillations caused by an initial number mismatch $\delta N_0/N = 0.1$ are shown in Fig. 4, center, for the parameters of Fig. 2. This figure also shows the number of normal atoms that have traveled through the constriction,

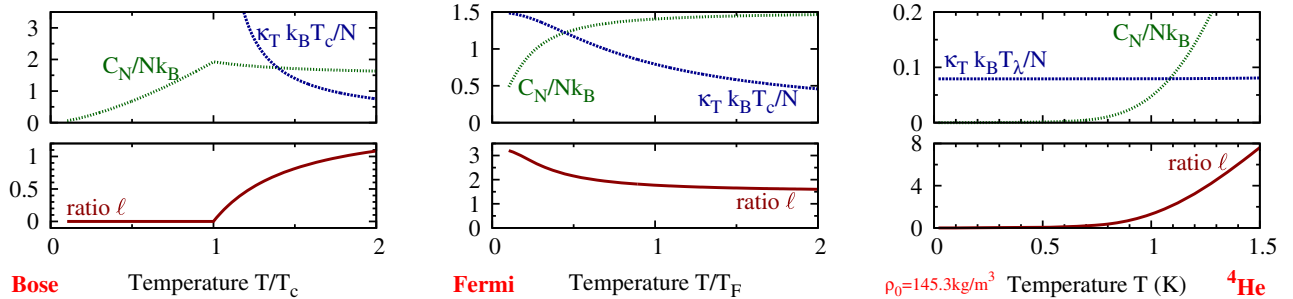


FIG. 3 (color online). Specific heat C_N (dotted green line), compressibility κ_T (dashed blue line), and their ratio ℓ (solid red line), for ideal Bose (left) and Fermi (center) gases, and for liquid helium 4 (right, density $\rho_0 = 145.3$ kg/m 3 , calculated using the data in Ref. [29]).

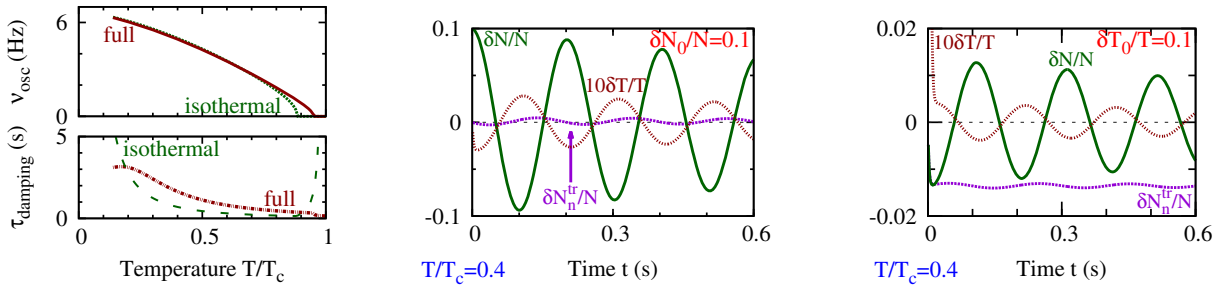


FIG. 4 (color online). Plasma oscillations in a ^{87}Rb gas, for the parameters of Fig. 2. Left: frequency $\nu_{\text{osc}} = \omega_{\text{osc}}/2\pi$ (top) and damping time τ_{damp} (bottom) for plasma oscillations at nonzero temperatures below T_c , calculated using Eq. (3) (red “full”) and its isothermal limit (dashed green “isothermal”). Center: the initial imbalance in atom numbers $\delta N_0/N = 0.1$ causes quasi-isothermal oscillations. Right: the initial temperature mismatch $\delta T_0/T = 0.1$ yields fast thermalization accompanied by an efficient transport of the thermal part at short times, followed by quasi-isothermal oscillations. In both cases, $T/T_c = 0.4$, and we plot $\delta N/N$ (solid green line), $\delta T/T$ (dotted red line, multiplied by 10), and $\delta N_n^{\text{tr}}/N$ (dashed purple line), as a function of time.

$\delta N_n^{\text{tr}}(t)$ [33], to reveal that these oscillations are performed almost exclusively by the superfluid part.

Thermalization at temperatures below T_c .—In order to reveal the key role played by fast thermalization in ultracold Bose gases, we now consider the response of the system to an initial temperature mismatch δT_0 . We consider temperatures $T/T_c \lesssim 0.5$. In this case, the dynamics of the system at small times of the order of τ_T is driven by the relaxation of temperature towards $\delta T = 0$. This fast process quickly converts the initial temperature mismatch δT_0 into a number imbalance δN_{max} ,

$$\frac{\delta N_{\text{max}}}{N} = \frac{15 \zeta(5/2)}{4 \zeta(3/2)} \frac{\mathcal{S}}{\mathcal{S}^2 + L} \left(\frac{T}{T_c}\right)^{3/2} \frac{\delta T_0}{T}. \quad (6)$$

The sign of δN_{max} is dictated by the Seebeck coefficient \mathcal{S} , which is negative, just like for fermions [6]. Furthermore, according to Eq. (1), temperature variations do not directly couple to the motion of the superfluid part. Hence, this fast relaxation process almost exclusively drives the transport of normal atoms. On a longer time scale, the oscillation then proceeds quasi-isothermally as before, with the frequency ω_{osc} and the damping time τ_{damp} . This process is illustrated in Fig. 4, right, for $\delta T_0/T = 0.1$ and the parameters used in Fig. 2. On the other hand, if a disordered potential is added to the system, the response to a temperature gradient $\delta T > 0$ will be very different from Fig. 4 (right). Assuming that the normal flow is blocked, the system will undergo plasma oscillations about a state of chemical equilibrium with $\delta N/N = -0.04$, in accordance with the thermomechanical effect predicted in Ref. [15].

Thermalization at temperatures above T_c .—In Bose gases, the ratio ℓ remains small for temperatures $T \gtrsim T_c$, where the physics is captured by the ideal-gas model and a direct comparison with fermions is possible (see Fig. 3, left and center). The gas contains no superfluid part, and the dynamics of δN and δT are described by the lower right 2×2 block of Eq. (3), which coincides with the model of Ref. [6]. Equation (4) shows that the

thermalization time τ_T is determined by the specific heat, which is of the same order of magnitude for Bose and Fermi gases. However, the damping time τ_1 involves the compressibility, which is much larger for bosons than for fermions. Therefore, damping is much slower in Bose gases than in Fermi gases. The variation of δN reflects the two time scales τ_T and τ_1 . In both cases, the Seebeck coefficient \mathcal{S} is negative; therefore, δN first decreases towards negative values. It reaches a minimum for short times $t_m \approx \tau_T \ln(\tau_1/\tau_T)$, whose value $\delta N_m \approx \delta T_0/TC_N \mathcal{S}/(\mathcal{S}^2 + L)$ does not depend critically on the statistics. However, the difference between bosons and fermions is apparent during the long-time relaxation towards $\delta N = 0$. Figure 5 compares the cases of bosonic ^{41}K at the temperature $T/T_c = 1.1$ and fermionic ^{40}K at the temperature $T/T_F = 1.1$, with T_F being the Fermi energy. These two isotopes differ only by the statistics which they obey, and the relaxation is 50 times longer for bosons ($\tau_1^B \sim 1.5$ s) than for fermions ($\tau_1^F \sim 30$ ms).

Strictly speaking, the plasma oscillations we have analyzed for $T < T_c$ are not Josephson oscillations. These would occur for $\mu \ll \hbar\omega_{\perp}$, which is opposite to our hydrodynamicity condition for the superfluid flow.

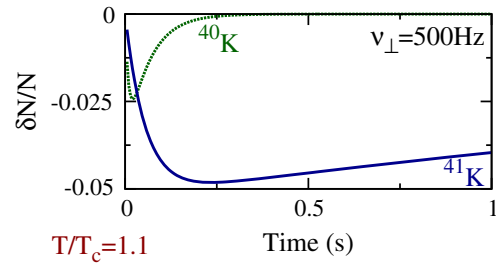


FIG. 5 (color online). Evolution of $\delta N/N$ following an initial temperature imbalance $\delta T_0/T = 0.1$ for bosonic ^{41}K (solid blue line, $T = 1.1T_c$) and fermionic ^{40}K (dashed green line, $T = 1.1T_F$). No superfluid is present, and the constriction is more stringent ($\omega_{\perp}/2\pi = 500$ Hz) to achieve bosonic decay times of the order of 1 s.

However, in the linear-response limit, the two equations determining the superfluid dynamics at $T = 0$ are formally equivalent to the Josephson equations (see Ref. [24], Chap. 15). A qualitative difference with true Josephson oscillations will emerge in the nonlinear regime, where deviations from the law $\Delta N_s = I_J \sin(\Delta\phi)$ should be seen. The classical-to-quantum crossover to Josephson oscillations can be explored numerically at $T = 0$ by varying the constriction geometry. Furthermore, if both μ and T are $\ll \hbar\omega_\perp$, the discretization of the channel conductance (recently observed in Fermi gases [8]) will play a key role.

In conclusion, we have shown that, in the case where the transport of the normal part is ballistic, plasma oscillations can be observed at nonzero temperatures below T_c , and that thermalization between the reservoirs is fast compared to the oscillation period, causing an efficient transport of the normal part at short times (see Fig. 4, right). A possible way to inhibit normal transport, and thus to realize a superleak, is to add a disordered potential inside the constriction, for instance by projecting a speckle [6], in analogy with the fine powders used in the historical superleaks [13]. The presence of disorder should not impede superfluid flow [34], but the normal flow will be dictated by a competition between conductance and disorder inside the channel, whose analysis in the fermionic case has been initiated in Ref. [6].

We are grateful to S. Balibar, I. Carusotto, G. Ferrari, and A. Georges for fruitful discussions. This work has been supported by the European Research Council (ERC) through the QGBE grant.

*Corresponding author.
papoular@science.unitn.it

- [1] E. L. Hazlett, L.-C. Ha, and C. Chin, [arXiv:1306.4018](#).
- [2] A. Rancon, C. Chin, and K. Levin, [arXiv:1311.0769](#).
- [3] F. Jendrzejewski, S. Eckel, N. Murray, C. Lanier, M. Edwards, C. J. Lobb, and G. K. Campbell, *Phys. Rev. Lett.* **113**, 045305 (2014).
- [4] J.-P. Brantut, J. Meineke, D. Stadler, S. Krinner, and T. Esslinger, *Science* **337**, 1069 (2012).
- [5] D. Stadler, S. Krinner, J. P. Brantut, and T. Esslinger, *Nature (London)* **491**, 736 (2012).
- [6] J. P. Brantut, C. Grenier, J. Meineke, D. Stadler, S. Krinner, C. Kollath, T. Esslinger, and A. Georges, *Science* **342**, 713 (2013).
- [7] J. G. Lee, B. J. McIlvain, C. J. Lobb, and W. T. Hill, III, *Sci. Rep.* **3**, 1034 (2013).
- [8] S. Krinner, D. Stadler, D. Husmann, J. Brantut, and T. Esslinger, [arXiv:1404.6400](#).
- [9] S. Krinner, D. Stadler, J. Meneike, J. Brantut, and T. Esslinger, [arXiv:1311.5174](#).
- [10] Y. V. Nazarov, *Quantum Transport: Introduction to Nanoscience* (Cambridge University Press, Cambridge, England, 2009).
- [11] C. Grenier, C. Kollath, and A. Georges, [arXiv:1209.3942](#).
- [12] B. T. Seaman, M. Krämer, D. Z. Anderson, and M. J. Holland, *Phys. Rev. A* **75**, 023615 (2007).
- [13] J. F. Allen and H. Jones, *Nature (London)* **141**, 243 (1938).
- [14] R. J. Donnelly, *Phys. Today* **62**, No. 10, 34 (2009).
- [15] D. J. Papoular, G. Ferrari, L. P. Pitaevskii, and S. Stringari, *Phys. Rev. Lett.* **109**, 084501 (2012).
- [16] L. D. Landau and E. M. Lifshitz, *Fluid Mechanics* (Pergamon, New York, 1987).
- [17] Y. Sato and R. E. Packard, *Rep. Prog. Phys.* **75**, 016401 (2012).
- [18] M. Albiez, R. Gati, J. Fölling, S. Hunsmann, M. Cristiani, and M. K. Oberthaler, *Phys. Rev. Lett.* **95**, 010402 (2005).
- [19] L. J. LeBlanc, A. B. Bardou, J. McKeever, M. H. T. Extavour, D. Jervis, J. H. Thywissen, F. Piazza, and A. Smerzi, *Phys. Rev. Lett.* **106**, 025302 (2011).
- [20] S. Giorgini, L. P. Pitaevskii, and S. Stringari, *Rev. Mod. Phys.* **80**, 1215 (2008).
- [21] L. A. Sidorenkov, M. K. Tey, R. Grimm, Y.-H. Hou, L. P. Pitaevskii, and S. Stringari, *Nature (London)* **498**, 78 (2013).
- [22] S. Datta, *Electronic Transport in Mesoscopic Systems* (Cambridge University Press, Cambridge, England, 1995).
- [23] K. Schwab, E. A. Henriksen, J. M. Worlock, and M. L. Roukes, *Nature (London)* **404**, 974 (2000).
- [24] L. P. Pitaevskii and S. Stringari, *Bose-Einstein Condensation* (Oxford Clarendon Press, Oxford, 2003).
- [25] Y. Kagan, D. L. Kovrizhin, and L. A. Maksimov, *Phys. Rev. Lett.* **90**, 130402 (2003).
- [26] I. Zapata and F. Sols, *Phys. Rev. Lett.* **102**, 180405 (2009).
- [27] The Landauer-Büttiker predictions for the normal current I_N and the entropy current I_S can be summarized as ([10], Chap. 1) $I_N = \int_0^\infty dE \Phi(E) (\eta_L^B - \eta_R^B) / h = L_{11} \delta\mu + L_{12} \delta(k_B T)$ and $I_S = \int_0^\infty dE \Phi(E) (s_L^B - s_R^B) / h = k_B [L_{21} \delta\mu + L_{22} \delta(k_B T)]$. Here $\Phi(E) = (E/\hbar\omega_\perp)^2/2$ is the number of open transport channels at energy E in the harmonic constriction, and $s^B(E) = k_B [(\eta^B + 1) \ln(\eta^B + 1) - \eta^B \ln \eta^B]$ is the entropy density associated with Bose statistics.
- [28] In Eq. (3), we have set to 0 the top right and lower left matrix coefficients. These coefficients are respectively equal to α/κ_T and $-(\omega_p \tau_1)^2 \alpha / (\kappa_T \ell)$, where $\alpha = \partial N / \partial T|_\mu$, and they have a negligible impact on the dynamics of the system. We have retained them in our numerical calculations.
- [29] V. D. Arp, *Int. J. Thermophys.* **26**, 1477 (2005).
- [30] W. H. Press, S. A. Teukolsky, W. T. Vetterling, and B. P. Flannery, *Numerical Recipes* 3rd ed. (Cambridge University Press, Cambridge, England, 2007)
- [31] F. Dalfovo and M. Modugno, *Phys. Rev. A* **61**, 023605 (2000).
- [32] A. L. Gaunt, T. F. Schmidutz, I. Gotlibovych, R. P. Smith, and Z. Hadzibabic, *Phys. Rev. Lett.* **110**, 200406 (2013).
- [33] The quantity $\delta N_n^{\text{tr}} = \int dt I_{N_n}$ differs from the difference in normal atom numbers δN_n because in each reservoir the normal fraction satisfies $N_n/N = (T(t)/T_c(t))^{3/2}$.
- [34] E. Lucioni, B. Deissler, L. Tanzi, G. Roati, M. Zaccanti, M. Modugno, M. Larcher, F. Dalfovo, M. Inguscio, and G. Modugno, *Phys. Rev. Lett.* **106**, 230403 (2011).